

Development of a Damping System that Reduce the Vibration of the Chandelier

Takahiro Kinoshita^{*1} Takayuki Sone^{*2} Masanori Iida^{*3}
Tsutomu Yokonami^{*4} Kenta Nagahama^{*5}

Summary

The authors proposed two types of damping systems that can reduce the response of chandeliers. The feature of these systems is that the energy dissipation system is placed only between the floor slab and the ceiling. Since this system is placed in the ceiling space, it does not distract from the appearance of the chandelier.

Shaking table tests of the proposed systems were performed and compared with the simulation by analytical model. The experimental results almost corresponded with the simulation by considering the effect of the friction of the dampers.

Keywords: chandelier, damping system, shaking table test, image analysis

1 Introduction

Damage to non-structural members is a form of seismic damage. The Great East Japan Earthquake, which occurred on March 11, 2011, caused large amounts of damage to ceilings and equipment^{1),2)}, and the need for securing the seismic resistance in non-structural members was recognized. Measures for the earthquake resistance of ceilings have been gradually systematized, but they remain insufficient for other non-structural members.

In this study, a damping method for chandeliers is proposed. Chandeliers are often installed in large spaces with an atrium or in living rooms with high ceilings, and they have a longer suspension length than other equipment. Cases where the natural period of the chandelier is close to that of the building may result in the chandelier resonating with the shaking of the building, resulting in significant shaking of the chandelier. As the damping capacity of the chandelier itself is also low, it shakes easily during earthquakes and takes a long time for the shaking to subside. The chandelier can make users of the building feel uneasy in the event of an earthquake, and in the worst-case scenario, the chandelier may fall and injure users.

Seismic measures for chandeliers include a method for suppressing shaking by installing a damping material shown in reference 3). This method affects the appearance of the chandelier because the chandelier itself needs to be fixed with a damping material. However, as chandeliers are largely valued for their aesthetics, such measures that affect their appearance are not desirable. The strength of the chandelier itself when such damping material is fixed may also be insufficient, and this measure is not considered effective.

Considering the facts mentioned, a damping system that could effectively add damping to the chandelier was devised. A feature of this system is that countermeasures are limited between the ceiling slab and ceiling material, which allows for the shaking to be effectively suppressed without disturbing the appearance of the chandelier. The following sections outline the proposed damping system and derive the equation of motion. Next, the conditions for minimizing the amplitude ratio of the fixed points of the transfer function are arranged based on the fixed points theory, and the effects are shown using the transfer function and time history response analysis. Finally, the effects of this system are verified by using a shaking table test, and the validity is verified by comparing with the analysis results. This system was developed mainly for chandeliers, but can also be applied to other suspended objects.

*1 Researcher, Research & Development Institute

*2 Chief Researcher, Research & Development Institute

*3 Manager, Design Department, Nagoya Branch Office

*4 Deputy Senior Manager, Design Department, Nagoya Branch Office

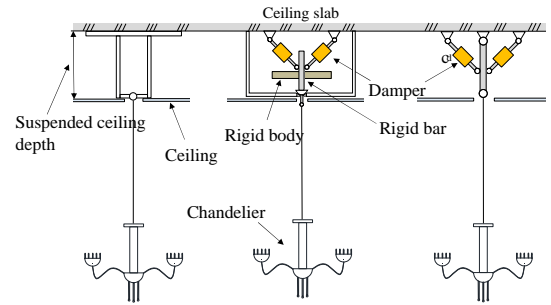
*5 Associate Chief Researcher, Research & Development Institute

2 Overview of the Damping System

2.1 Damping System Configuration

Figure 1(a) shows an outline of the installation of a conventional chandelier. Conventional methods commonly hung a chandelier with a chain from a stand set up in a ceiling pocket. The chain itself does not have a damping capacity, thus a long time elapses before the shaking subsides. In contrast, the proposed system has a configuration in which shaking is absorbed by a damper provided between the ceiling slab and ceiling material, as shown in Figs. 1(b) and (c).

The system in Fig. 1(b) (damping system 1) consists of a rigid bar, rigid body, and a damper, and it has a support point that uses a pin joint near the ceiling material. This system requires the rigid body shape to be designed such as to obtain an appropriate moment of inertia. The system in Fig. 1(c) (damping system 2) is a simplified version of damping system 1. A characteristic of this system is that the stand used in the damping system 1 does not need to be installed because this system does not have a rigid body installed and the support point for pin jointing is provided near the ceiling slab. In addition, its damping effects compared to damping system 1 are smaller because there are no moment of inertia effects of the rigid body.



(a) Conventional (b) Damping system 1 (c) Damping system 2

Fig.1 Outline of the systems

2.2 Equation of Motion for Damping System 1

Figure 2(a) shows a model diagram of damping system 1. The chandelier is treated as a pendulum with a single point mass. Considering the balance of moments around point O_1 and setting $\theta_1 \approx 0$, then Eq. (1) is derived.

$$M_1 \ddot{x}_1 + K_1(x_1 - x_2) = -M_1 \ddot{y}_0 \quad (1)$$

Here, $M_1 = m_1$ and $K_1 = m_1 g / L_1$, and it is assumed that there is no attenuation in the chandelier.

Next, considering the balance of moments around O_2 and setting $\theta_1 \approx 0$ and $\theta_2 \approx 0$, then Eq. (2) is obtained.

$$M_2 \ddot{x}_2 + C_2 \dot{x}_2 - K_1(x_1 - x_2) + K_2 x_2 = -\eta M_2 \ddot{y}_0 \quad (2)$$

Here, $\alpha = -L_3 / L_2$, $\beta = L_1 / L_2$, $M_2 = \alpha^2 m_2 + I_2 / L_2^2$, $K_2 = \alpha m_2 g / L_2 + \beta K_1$, $\eta = \alpha m_2 / M_2$, and $C_2 = 2C_d \cos^2 \varphi_1 (L_4 / L_2)^2$. Equation (3) can be obtained by expressing Eqs. (1) and (2) in the form of an equation of state.

$$\begin{Bmatrix} \dot{x}_1 \\ \dot{x}_2 \\ \ddot{x}_1 \\ \ddot{x}_2 \end{Bmatrix} = \begin{bmatrix} 0 & I \\ -M^{-1}K & -M^{-1}C \end{bmatrix} \begin{Bmatrix} x_1 \\ x_2 \\ \dot{x}_1 \\ \dot{x}_2 \end{Bmatrix} + \begin{Bmatrix} 0 \\ 0 \\ 1 \\ \eta \end{Bmatrix} \ddot{y}_0 \quad (3)$$

Here, $M = \begin{bmatrix} M_1 & 0 \\ 0 & M_2 \end{bmatrix}$, $C = \begin{bmatrix} 0 & 0 \\ 0 & C_2 \end{bmatrix}$, and $K = \begin{bmatrix} K_1 & -K_1 \\ -K_1 & K_1 + K_2 \end{bmatrix}$. Furthermore, O and I are 2×2 zero and identity matrices, respectively.

2.3 Equation of Motion for Damping System 2

Figure 2(b) shows a model diagram of damping system 2. As in the damping system 1, the chandelier is considered a pendulum with a single point mass. Considering the balance of moments around O_1 and setting $\theta_1 \approx 0$, then Eq. (4) is derived.

$$-M_1(\ddot{x}_1 + \ddot{y}_0) = K_1(x_1 - x_2) \quad (4)$$

Here, $M_1 = m_1$ and $K_1 = m_1 g / L_1$, and it is assumed that there is no attenuation in the chandelier.

Next, considering the balance of moments around O_2 and setting $\theta_1 \approx 0$ and $\theta_2 \approx 0$, then Eq. (5) is obtained.

$$-M_1(L_1 + L_2)(\ddot{x}_1 + \ddot{y}_0) = C_2' L_2 \dot{x}_2 + M_1 g \dot{x} \quad (5)$$

Here, $C_2' = 2C_d \cos^2 \varphi_1 (L_3/L_2)^2$.

Substituting Eq. (4) into Eq. (5) and eliminating the $(\ddot{x}_1 + \ddot{y}_0)$ term, and expressing this and Eq. (4) in the form of an equation of state results in Eq. (6).

$$\begin{cases} \dot{x}_1 \\ \dot{x}_2 \\ \ddot{x}_1 \end{cases} = \begin{bmatrix} 0 & 0 & 1 \\ K_1/C_2' & -(\beta + 1)K_1/C_2' & 0 \\ -K_1/M_1 & K_1/M_1 & 0 \end{bmatrix} \begin{cases} x_1 \\ x_2 \\ \dot{x}_1 \end{cases} + \begin{cases} 0 \\ 0 \\ 1 \end{cases} y_0 \quad (6)$$

Here, $\beta = L_1/L_2$.

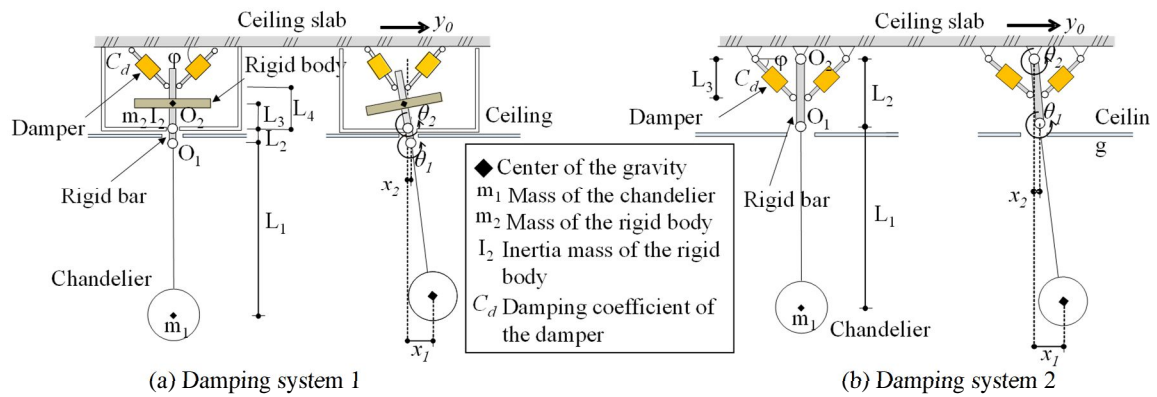


Fig.2 Diagram of the systems

3 Investigation of Optimal Parameters Based on Fixed Points Theory

The transfer function of the entire system obtained from Eqs. (3) and (6) has fixed points at which the amplitude ratio with respect to the harmonic motion becomes a constant value at a certain angular frequency, regardless of the damping coefficients (C_2 , C_2'). The existence of such fixed points is known as the fixed points theory⁴⁾. In this section, the parameters for realizing the optimal state defined for each system are derived based on the fixed points theory. In the following sections, the damping coefficients obtained by the damper (C_2 from Eq. (3), C_2' from Eq. (6)) will be expressed in a unified manner as the damping coefficient C .

3.1 Optimal Parameters of Damping System 1

The optimal state of damping system 1 is defined as the state where the maximum amplitude ratio value of the transfer function is minimized by setting an appropriate damping coefficient while the magnitudes of the amplitude ratios at the two fixed points obtained based on the fixed points theory are aligned. The conditions are derived as follows.

The steady-state response by the harmonic motion $y_0 = Y_0 e^{i\omega t}$ of the ceiling slab is set to $x_1 = X_1 e^{i\omega t}$ and $x_2 = X_2 e^{i\omega t}$. Considering the amplitude ratio $|X_1/Y_0|$ to the amplitude Y_0 , there is a fixed point where the amplitude ratio $|X_1/Y_0|$ is constant for a certain angular frequency ω regardless of the value of the damping coefficient C . The values of the angular frequency ω and amplitude ratio $|X_1/Y_0|$ at this time can be obtained by Eqs. (7) and (8).

$$\text{When } \omega = \sqrt{\frac{(\mu + \varphi) \pm \sqrt{(\mu - \varphi)^2 + 2\mu}}{2\mu}} \omega_1,$$

$$|X_1/Y_0| = |(\mu - \varphi + 1) \pm \sqrt{(\mu - \varphi)^2 + 2\mu}| \quad (7)$$

When $\omega = \sqrt{1 + \frac{1}{\eta\mu}} \omega_1$,

$$|X_1/Y_0| = \eta\mu + 1 \quad (8)$$

Here, $\omega_1 = \sqrt{K_1/M_1}$, $\omega_2 = \sqrt{K_2/M_2}$, $\Psi = \omega_2/\omega_1$, $\mu = M_2/M_1$, and $\varphi = (2\mu\Psi^2 + \eta\mu + 2)/2$. The two fixed points according to Eq. (7) are called points P and Q, and the fixed point in Eq. (8) is called point R.

The condition where the amplitude ratios of points P and Q have the same magnitude is $\mu - \varphi + 1 = 0$ by Eq. (7), which can be arranged and expressed by Eq. (9).

$$\psi = \sqrt{1 - 0.5\eta} \quad \eta < 2 \quad (9)$$

The value of the fixed point when this condition is satisfied is expressed by Eq. (10).

$$(\omega, |X_1/Y_0|)_{P,Q} = \left(\sqrt{\frac{(2\mu+1) \pm \sqrt{(2\mu+1)}}{2\mu}} \omega_1, \sqrt{(2\mu+1)} \right) \quad (10)$$

When the relationship of $\eta\mu + 1 < \sqrt{2\mu+1}$ is valid, the amplitude ratio of Eq. (10) is larger than the amplitude ratio of point R in Eq. (8). When the values of $m_1, m_2, L_1, L_2,$ and L_3 are determined, the value of the moment of inertia I_2 required to satisfy Eq. (9) can be obtained from Eq. (11).

$$I_2 = m_1 L_1 L_2 + m_2 (L_1 + 0.5L_2 - L_3) L_3 \quad (11)$$

The transfer characteristic that minimizes the maximum amplitude ratio value of the transfer coefficient can be achieved when the above equation is satisfied and an appropriate damping coefficient C is given. The derivation of this damping coefficient C is complex, thus it was numerically computed in this study.

3.2 Optimal Parameters of Damping System 2

The optimal state of damping system 2 is defined as the state that minimizes the amplitude ratio of one fixed point obtained on the basis of the fixed points theory. Its conditions are derived below. In Eq. (6), the steady-state response by the harmonic motion $y_0 = Y_0 e^{i\omega t}$ of the ceiling slab is set as $x_1 = X_1 e^{i\omega t}$ and $x_2 = X_2 e^{i\omega t}$. When considering the amplitude ratio $|X_1/Y_0|$ to the amplitude Y_0 , there is a fixed point where the value of the amplitude ratio $|X_1/Y_0|$ is constant for a certain angular frequency ω regardless of the value of the damping coefficient C. The values of the angular coefficient ω and amplitude ratio $|X_1/Y_0|$ at this time are obtained from Eq. (12).

$$\omega = \sqrt{1 - 0.5/(\beta + 1)} \omega_1 \quad (12a)$$

$$|X_1/Y_0| = 2\beta + 1 \quad (12b)$$

Here, $\omega_1 = \sqrt{K_1/M_1}$.

Additionally, the fixed point according to Eq. (12) is called point P. Here, the damping coefficient for minimizing the amplitude ratio of the fixed point can be obtained with Eq. (13) from the condition in which the extreme value of the transfer function with respect to the frequency ω of the fixed point P matches Eq. (12b).

$$C = (1 + \beta) \sqrt{\frac{2\beta}{2\beta+1}} \omega_1 M_1 \quad (13)$$

4 Analytical Investigation of Damping Effects

In this section, the characteristics of this system are confirmed using the transfer function of the study model, and the damping effects are verified by time history response analysis.

4.1 Study Model and Transfer Function

Table 1 shows the properties of the study model. The mass of the chandelier was 15 kg, and the suspension length was 1,570 mm. The rigid body mass in damping system 1 was twice the mass of the chandelier, and the moment of inertia value obtained from Eq. (11) was used.

Table 1 Property of study model

Property	m ₁ (kg)	m ₂ (kg)	L ₁ (mm)	L ₂ (mm)	L ₃ (mm)	φ (°)
Damping system 1	15	30	1570	200	70	45
Damping system 2		-		600	300	

The damping coefficient C was also numerically computed such that the characteristics were close to the optimal state.

Figure 3 shows the transfer function. The solid black line indicates the case when the damping coefficient is C = ∞ (pendulum with suspension length L₁), and the dotted black line shows when C = 0 (pendulum with suspension length L₁+L₂). As shown in Fig. 3(a), the fixed points of damping system 1 coincide with the two intersections of the transfer functions for C = 0 and C = ∞. The transfer function in the optimal state shown with the red line has transfer characteristics whose amplitude ratio near the fixed points is maximized at the same height where the amplitude ratios |X₁/Y₀| of these two intersections are at the same height. As shown in Fig. 3(b), the fixed point of damping system 2 (point P) coincides with the intersection of the transfer functions for C = 0 and C = ∞. The amplitude ratio at that fixed point for the transfer function in the optimal state shown by the red line is maximized in the entire frequency domain.

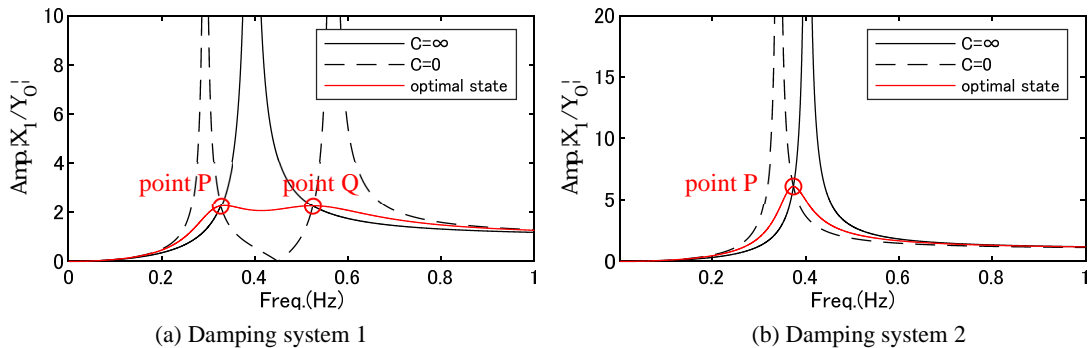


Fig.3 Transfer function

4.2 Time History Response Analysis

The input wave to the study model is the response wave of the building model. The building model is an equivalent shear model assuming the short side direction of the 24-story S-structured hotel shown in reference 5). The first-order natural period in the short side direction is 2.55 s, which is close to the natural period of the chandelier (2.51 s), and response amplification due to resonance is assumed in the chandelier.

The JMA Kobe of the 1995 Great Hanshin Earthquake (NS direction)⁶⁾ and the Ministry of Land, Infrastructure, Transport and Tourism base adjustment wave CH1⁷⁾ were adopted as the seismic motion inputs into the building model. The response wave on the fourth floor obtained from the time history response analysis of the building model was used as the input wave into the study model. This input assumes a chandelier that could be seen from the lobby in the lower section of a typical hotel. The input waves into the study model are shown in Fig. 4.

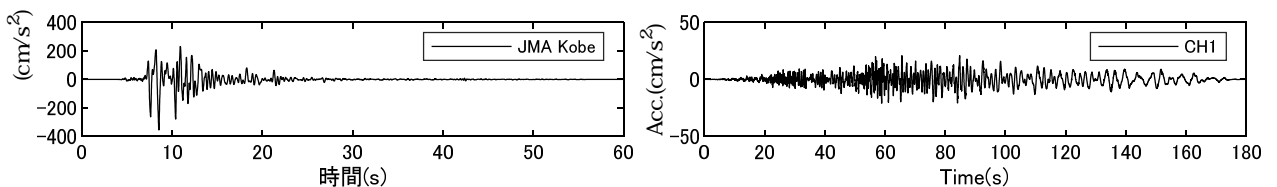


Fig.4 Input waves to the studied model

Figure 5 shows the displacement waveform of the chandelier obtained from the time history response analysis. The single point mass model simulating a conventional chandelier without countermeasures ($h = 0.5\%$) was also analyzed as a comparison. The maximum displacement reduction rate in damping system 1 was approximately 45% in JMA Kobe and approximately 85% in CH1. In addition, the maximum displacement reduction rate in damping system 2 was approximately 18% in JMA Kobe and approximately 61% in CH1. As shown in these results, the effects were higher in damping system 1. When focusing on differences due to the nature of the seismic motion, it was observed that the effect on CH1, which is a long-period ground motion, was higher than on JMA Kobe, which is a pulsed ground motion, with the damper functioning more effectively.

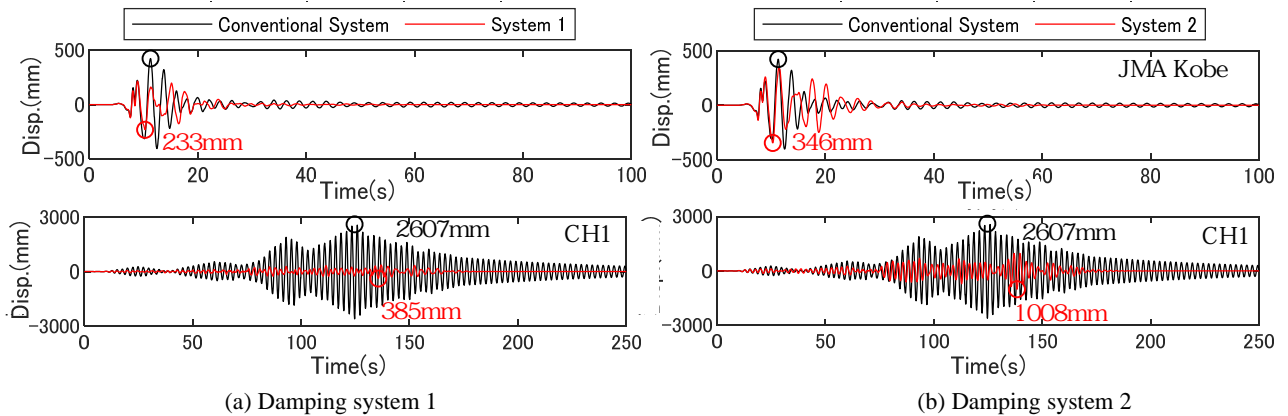


Fig.5 Analysis results

5.1 Outline of Specimen

Figures 6 and 7 show the outlines of the specimen. The specimen was configured to satisfy the properties in Table 1. The main components of damping system 1 were the chandelier, rigid body, rigid bar, spherical bearings, and oil damper. Two H-steels were attached to the steel frame at the same level, and an iron plate with a $\phi 50$ hole in the center was attached on top of it. A spherical bearing was installed on this iron plate to construct a pin joint corresponding to the point O_2 in Fig. 2. The main components of damping system 2 were the chandelier, rigid bar, and oil damper. A commercially - available single-effect type that exerts a damping force only in the tensile direction was used for the oil damper, which is common for both systems, after considering the cost at the time of practical deployment. Two dampers, which operated in both directions, were installed. The damping coefficient C was adjusted for the damping force of the damper and the installation angle / position such as to be approximately equal to the value in the optimal state.

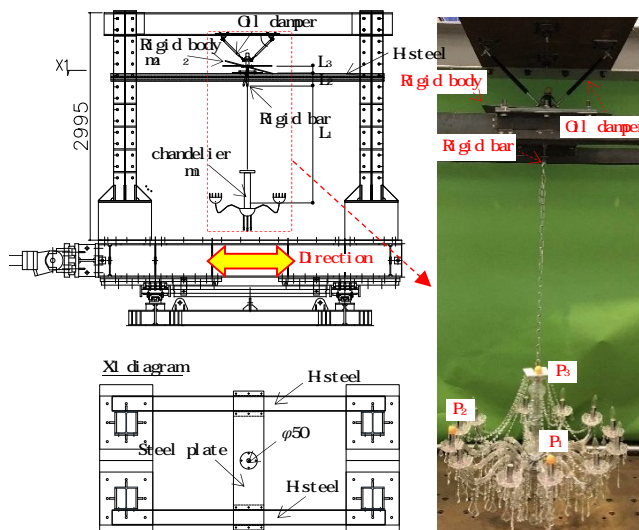


Fig.6 Outline of specimen (system 1)

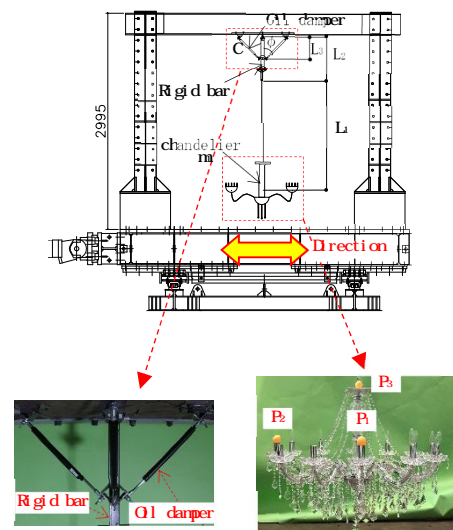


Fig.7 Outline of specimen (system 2)

The performance of the damping characteristics of the damper was confirmed by applying sine waves of various frequencies and amplitudes. Figure 8 shows the load-displacement relationship when a 0.4-Hz sine wave was applied as a typical example. The tensile direction of the damper was +, and the compressive direction was -. It could be seen that a load of approximately 10 N was generated in the compressive direction. Figure 9 shows the velocity obtained from the first derivative of the displacement and expressed in the form of the load-velocity relationship. A load of approximately 10 N was generated after a movement in the compressive direction, which is presumed to be the effect of friction. In addition, the damper had almost linear characteristics in the tensile direction.

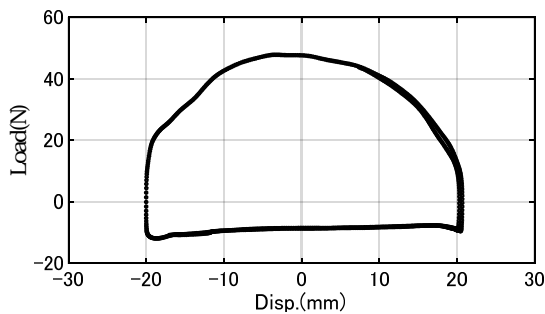


Fig.8 Relationship between load and displacement of the damper

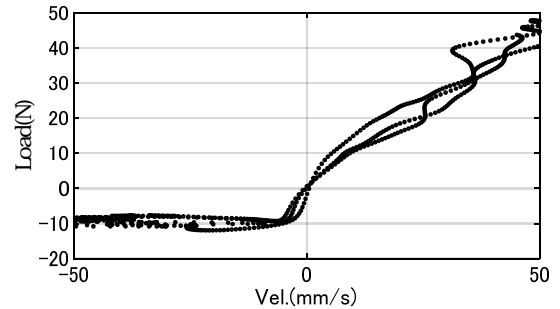


Fig.9 Relationship between load and velocity of the damper

5.2 Excitation Outline, Implementation Case, and Measurement Outline

Uni-directional excitation was conducted in the direction shown in Figs. 6 and 7 using a 1,000-kN actuator attached to a shaking table. The excitation wave was set as the response wave (JMA Kobe, CH1) of the fourth floor of the building model described in the previous section. The input level of each excitation wave was adjusted such that the maximum displacement of the chandelier without countermeasures (specimen that was fixed to impede movement by replacing the damper section with an angle material) was approximately 200 mm. There were three implementation cases: damping system 1, damping system 2, and no countermeasures.

In this experiment, the displacement of the chandelier was measured using image analysis. The target used for image analysis was P₂ in Figs. 6 and 7, where the effects of rotation in the plane of the chandelier were minimal, and whose height was close to the position of the center of gravity. TAMA 2D was used for image analysis. The measurement camera had a screen resolution of 1,980 × 1,080, the field of view was narrow, and the frame rate was 60 fps. Lens calibration was performed before the experiment at the angle of view to be measured.

5.3 Experimental Results of Damping System 1

Figure 10 shows a comparison of the experimental results between damping system 1 and no countermeasures. Comparisons of the maximum deformation show the response reduction effects due to this system, but the damping tendencies of the free vibration part were approximately equal to the case where no countermeasures were taken. Considering the effects of friction seen in the compressive direction of the damper, the damping capacity of the damper may not be effectively expressed when the chandelier shaking is small. Therefore, Fig. 11 shows a comparison between the analysis results and experimental results when considering

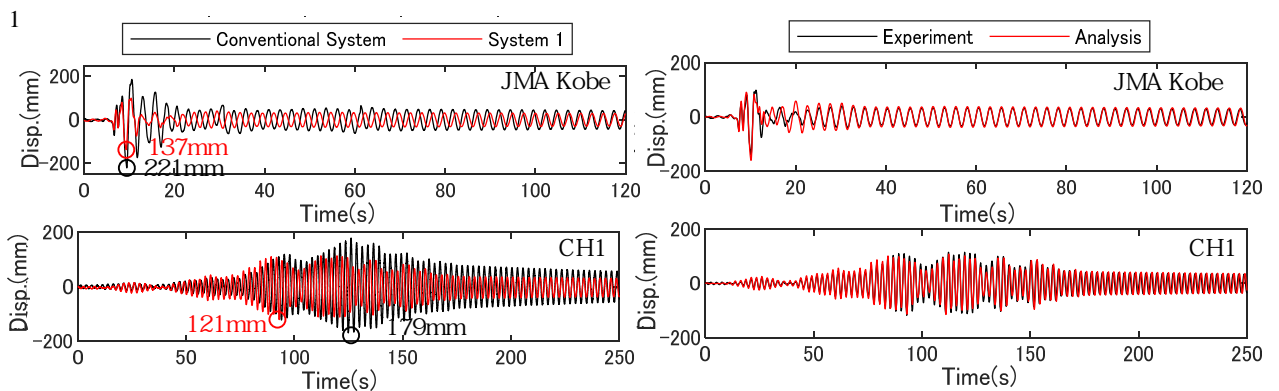


Fig.10 Comparison of experiment results

Fig.11 Comparison of experiment and analysis

the friction of the damper. It can be seen that the phase and maximum displacement of the free vibration part could be effectively reproduced by analysis.

5.4 Experimental Results of Damping System 2

Figure 12 shows a comparison of the experimental results between damping system 2 and no countermeasures. Comparisons of the maximum deformation showed that the JMA Kobe results had a small effect, but that the CH1 decreased the value to approximately half. Moreover, the expected effects may have been insufficiently obtained during small amplitudes, similar to the case in damping system 1, due to the friction effects of the damper.

It was mentioned in the previous section that the experiment and analysis results were consistent with each other by considering the effects of friction in the analysis. Similar tendencies could be confirmed in damping system 2 as well, but comparisons by the transfer function are also important for confirming the characteristics of specimens. However, the time of the free vibration part was extremely long due to the friction effects of the damper, and the transfer function could not be clearly obtained from the fast Fourier transform of the displacement waveform. Therefore, the shaking table was vibrated with a sine wave in damping system 2, and the transfer function was obtained from the displacement ratios of the chandelier and shaking table when the specimen was in a steady state. This was then compared with the analysis results. The frequency of the sine wave fluctuated from 0.2 to 0.5 Hz in 0.01-Hz increments. Figure 13 shows the transfer function obtained from analyses and the experimental results. The experimental results could effectively reproduce the specimen characteristics, and it was confirmed that they were consistent with the theoretical values when the amplitude of the chandelier was large and the friction effects were relatively small.

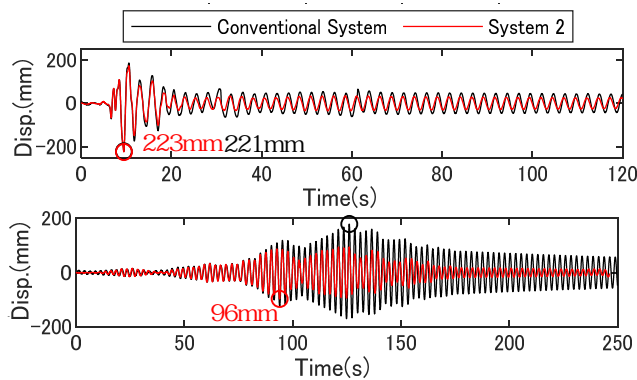


Fig.12 Comparison of experiment results

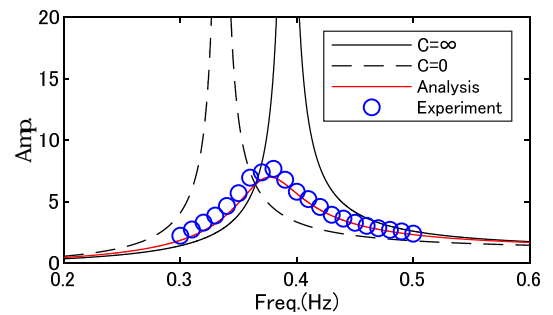


Fig.13 Comparison of transfer function

6 Analytical Investigation of Damping Effects Considering Frictional Force of Damper

The investigations in the previous section confirmed that the response of the chandelier could be appropriately evaluated by considering the effect of friction of the damper. In addition, the displacement of the chandelier when no countermeasures were implemented had its input level lowered such that the displacement would be approximately 200 mm, thus it was considered that there was a relatively large effect of friction on the start of movement. In this chapter, the input wave of the actual response wave level used in Section 4.2 was used to analyze whether the effect of friction would be problematic at large amplitude levels.

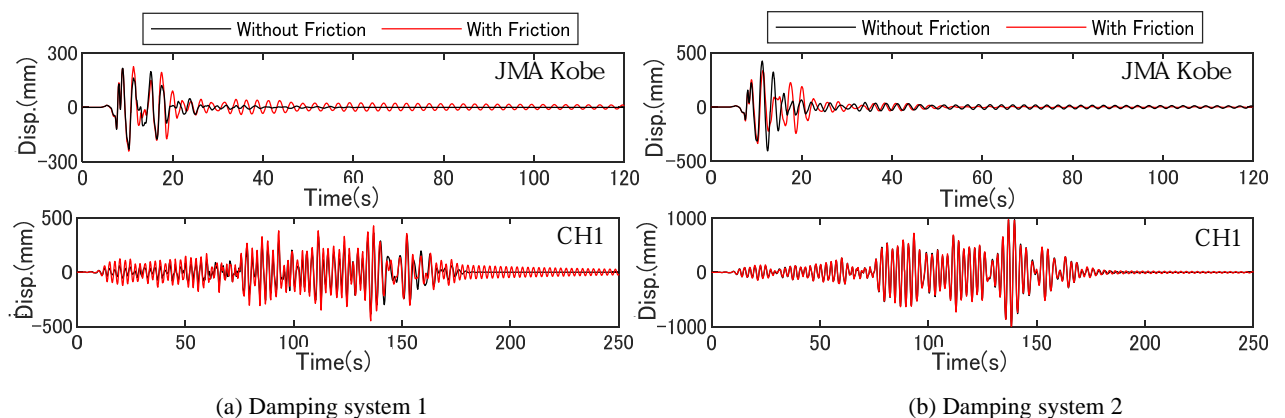


Fig.14 Comparison of analysis results

Figure 14 shows a comparison of the analysis results with and without the friction of the damper. The input ground motion was set as a response wave on the fourth floor of the building model used in Section 4.2. There were no major differences in the response in damping system 1 compared to when the large amplitude part was not considered, but the effect of friction was large in the small amplitude part, represented by the free vibration part. This tendency did not change for damping system 2 as well. The effect assumed in the analysis could be expected in the large amplitude area considering the friction level of the damper used in this study.

7 Conclusions

In this report, a damping system that reduces the shaking during an earthquake without negatively affecting the aesthetic appearance of a chandelier is proposed. The damping effects were verified using a time history response analysis and shaking table test. The conclusions are shown below.

- (1) The equations of motion for the two proposed damping systems are shown, and the parameters that are in the optimal state are shown for each of the equations;
- (2) Investigations of the damping effects by time history response analysis showed that the effects on the long-period ground motion of CH1 were higher than on the pulsed ground motion of JMA Kobe. The maximum displacement reduction rate at this time was approximately 85% at its highest;
- (3) The shaking table test and analysis results were compared. The friction effects of the damper in the analysis effectively captured the experimental result tendencies;
- (4) The friction effects of the damper were confirmed to be minimal in the large amplitude area based on analytical investigations of the actual response wave level. It is considered that using a damper with small frictional force increased the damping effects at small amplitudes. In addition, the optimal damper should be selected considering the cost-effectiveness and the cost of the chandelier.

References

- 1) Architectural Institute of Japan: Great East Japan Earthquake Joint Survey Report, Architecture Edition 6, Non-Structural Members, 2019.
 - 2) Architectural Institute of Japan: Research on the Mitigation of Damage by Earthquakes and Wind on Non-Structural Members (Roof, Outer Wall, Ceiling), 2008.
 - 3) Japan Building Equipment and Elevator Center Foundation: Building Equipment / Elevator Seismic Diagnosis Standards and Repair Guidelines, 1996.
 - 4) J. P. Den Hartog: Mechanical Vibration, 4th edition, McGraw-Hill, New York, 1956
 - 5) T. Kinoshita, et al.: PROPOSAL OF DAMPING SYSTEMS FOR CHANDELIERS. 16th World Conference on Seismic Isolation, 1-6 July 2019, Saint Petersburg, Russia
 - 6) Japan Meteorological Agency: Strong Earthquake Waveform (1995 Great Hanshin Earthquake), https://www.data.jma.go.jp/svd/eqev/data/kyoshin/jishin/hyogo_nanbu/index.html (last accessed 2020.08.05).
 - 7) Building Research Institute: Special Page for Disclosure of Technical Materials / Data related to Long-Period Ground Motion Countermeasures, <https://www.kenken.go.jp/japanese/contents/topics/lpe/index.html> (last accessed 2020.08.05).
-